

Origin of the Endo/Exo Stereoselectivity and Syn/Anti Face-Selectivity in Diels–Alder Reactions, Determined by Transition State Energy Partitioning

Shingo Kiri, Yuka Odo, Huda Izzat Omar, Tetsuro Shimo, and Kenichi Somekawa*

Department of Applied Chemistry and Chemical Engineering, Faculty of Engineering, Kagoshima University, 1-21-40, Korimoto, Kagoshima 890-0065

Received January 15, 2004; E-mail: some@apc.kagoshima-u.ac.jp

The origins of stereo- and face-selective Diels–Alder reactions of 5-substituted 1,3-cyclopentadienes (CP) with some dienophiles were elucidated by means of semiempirical PM5, DFT(B3LYP), and ab initio RHF methods. The activation energies by the improved PM5 and B3LYP/6-31+G(d) methods were in good agreement with the experimental results. We partitioned the activation energy (ΔE_{act}) into diene deformation ($\Delta E_{df\text{-}dien}$) and dienophile deformation ($\Delta E_{df\text{-}dphil}$), and the diene–dienophile interaction (E_{int}) energies, in addition to the new intrinsic reaction coordinate (IRC) energy (ΔE_{irc}) partitioning. Such analysis revealed the major factors in the determining endo/exo and syn/anti selectivities of the reactions of 5-substituted CP. The syn-selectivity of the 5-F-CP is explained by the lower ΔE_{act} (2–3 kcal/mol) caused by relatively smaller $\Delta E_{df\text{-}dien}$, which leads to slighter repulsion between the reactants. This low activation energy is inferred to be caused by the better second orbital interaction or intramolecular orbital interactions between the diene π and fluoro-substituent n orbital moieties, as well as by better intermolecular π–π orbital interactions between the diene-π and dienenophile-π moieties. On the other hand, the anti-selectivity of the methyl substituted CP mainly appears from bigger $E_{df\text{-}dien}$ in the syn-isomer. A novel economical method of IRC energy partitioning to the reactants, TS intermediates and products is also introduced in order to verify the energy balance of other calculation methods and other reactions.

The Diels–Alder (DA) reaction that produces some stereoselective adducts of versatile six-membered rings[1] is one of the most useful cycloaddition reactions in both theoretical and synthetic aspects. The endo/exo stereoselectivity of many DA reactions has been qualitatively explained by the non-bonding secondary orbital interactions (SOI) between dienes and a variety of substituted dienophiles.[2] Cossio et al. recently estimated that the SOI at the endo-DA reaction between 1,3-cyclopentadiene (CP) and maleic anhydride (MA) is −1.48 kcal/mol by the DFT(B3LYP/6-31G*) method.[3] The syn/anti facial selectivity for DA reactions of CP possessing a substituent such as a fluorine and C(=O) YR at the position 5 was predicted on the basis of the orbital mixing rule between the diene π orbital and the 5-substituent n orbital.[4] The selectivity was disclosed at the RHF/6-31G* level of calculation along with the experimental observations, to be highly dependent on the relative intramolecular orbital energy between the π_{homo} of the diene and the substituents $n_{F,Y}$ orbitals.[5] Burnell et al. also predicted the facial selectivities in the DA reactions of 5-substituted CP with a variety of dienophiles at the ab initio HF/6-31G* level of calculation.[6] Their calculations of activation energies for syn- and anti-cycloadditions, and their partitioning of the activation energy into diene deformation, dienophile deformation, and diene–dienophile interaction energies showed that the major factor affecting the selectivity is the energy required to deform the diene into its transition state (TS) geometry. The calculated activation energies were, however, higher than the experimental values: for example, it was over 15 kcal/mol higher in the typical DA reaction between CP and MA. The calculation results at the HF/6-31G* level may require some corrections for quantitative usage.

The B3LYP/6-31G* method was applied to study the DA reaction mechanism of 1,3-butadiene and ethylene. The energies of reactions and the geometries of the reactants and products are in good agreement with available experimental results, in comparison with those obtained by other calculation methods.[7,8] On the other hand, the DFT method was reported to have some problems concerning the structure analysis of [10]anullene, compared to the results from the high-performance CCSD(T) method that takes a long time for the calculations,[9] and the results from the reactivity analysis of the DA reactions of D-glucose-derived dienophiles with CP.[10] Recently, Domingo et al. studied the TS structures for a series of related DA reactions between CP and acrylonitriles with use of B3LYP/6-31G*.[11] This study was in accordance with the experimental outcome and explained the synchronicity on the newly forming bonds of these cycloadditions. Afarinkia et al. also studied the regio- and stereo-chemical preferences of the DA cycloadditions of 2H-pyran-2-ones using the B3LYP/6-31G*//AM1 method; this study allowed prediction of the selectivity quantitatively.[12]

Our team has used successfully some FMO calculations to investigate the peri-, site-, regio-, and/or stereoselective photocycloaddition reactions of 2-pyrones, 2-pyridones, and cyclic enones.[13] We have also used TS calculations to analyze site- and stereo-selective [2 + 2] photocycloadditions between some

Published on the web August 6, 2004; DOI 10.1246/bcsj.77.1499

2-pyrones and maleimide in the solid state by the PM3 method.[14] In addition we have inferred the origin of the drastic change in hh/ht regioselectivity in [2 + 2] photocycloaddition reactions of 2-cyclohexenone with cycloalkenecarboxylates by TS analysis using improved PM5 and B3LYP/6-31G* methods.[15] The PM5 levels were recognized to have balance in electron repulsions good enouph to estimate the transition state behaviors at cycloaddition reactions.

In this study, different calculation levels have been utilized to investigate the regio- and face-selectivities for two Diels–Alder reactions: the reactions of cyclopentadiene (CP) with maleic anhydride (MA) and the reactions of 5-substituted CP with acrylonitrile (AN). The former reaction has mainly produced a stereo-selective endo product (Scheme 1), and the latter showed syn-selectivity for the fluoro-substituted CP, and anti-selectivity for the 5-methyl substituted CP (Scheme 2). Symmetrical CP reactions are also well addressed in this research. Interestingly, we report herein the origin of endo/exo stereo- and syn/anti face-selectivities in those typical DA reactions. These reaction selectivities are quantitatively inferred from the possibility of partitioning the activation energy into reactant deformation energies (which are the energies required to deform the reactants into their transition state structures) and the interaction energy, by employing the PM5 method together with the B3LYP/6-31+G(d) method. Moreover, we present here a novel partitioning of the intrinsic reaction coordinate (IRC) surface energy[16] in which each energy barrier on the IRC surface is partitioned into two deformed components (reactant and product) and diene–dienophile interaction energies. The method may give much valuable information for the analysis of the reaction mechanisms in the future.

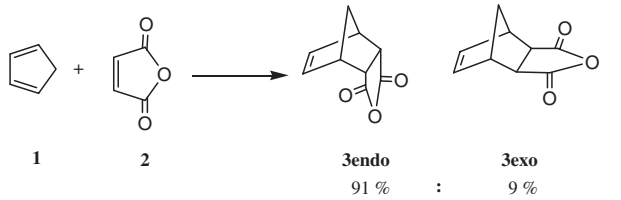

Scheme 1.

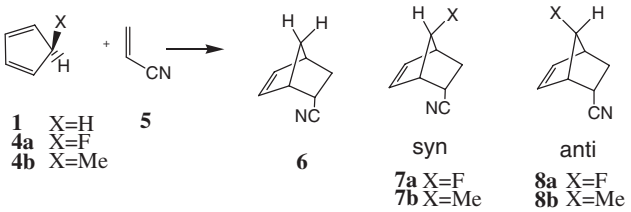

Scheme 2.

Computational Methods

Geometrical optimization of all molecules was carried out using the improved PM5[17] method in WinMOPAC 3.5 (Fujitsu Ltd[18]). The geometry was reoptimized by RHF[19] and B3LYP[20] methods, available in the Gaussian 98 program, on the standard basis set.[19] The TS analysis and the deformation energy analysis obtained by partitioning the activation energy (ΔE_{act}) into the reactant deformation energies ($\Delta E_{df\text{-}dien}$, $\Delta E_{df\text{-}dphil}$) and the diene–dienophile interaction energy (E_{int})[6] were investigated using the PM5 and B3LYP/6-31+G(d) methods. The ΔE_{df} is the energy required to change the reactant geometry into the transition state geometry. The E_{int} value is defined as ($\Delta E_{act} - (\Delta E_{df\text{-}dien} + \Delta E_{df\text{-}dphil})$). In efforts to circumscribe control of the selectivity more clearly, the partitioning of the IRC energy (ΔE_{irc}) into the two deformed reactants (or product) and diene–dienophile interaction energies along with the DA reaction was performed similarly at the TS point using the PM5 method and by single-point B3LYP/6-31+G(d) calculations.

Results and Discussion

DA Reactions of CP and MA. Experimental results in Scheme 1 show endo preference in the typical endo/exo stereoselectivity of the DA reaction between CP and MA. Various calculation methods were used to estimate the activation energy for both endo and exo reactions. The calculated and experimental results are shown in Table 1. The activation energy (ΔE_{act}) for the endo preference was 2.28, 1.40 kcal/mol lower than that for the exo product, using PM5 and the optimized B3LYP methods, respectively. Moreover the ΔE_{act} values estimated from those two methods were in accordance with the experimental results. In contrast, the ΔE_{act} values computed by AM1, PM3, and RHF/6-31G* were much higher than the experimental data.[7a,18] Therefore we assume that these methods are not efficient in explaining the endo preference of the reaction. The TS optimized structures, TS distances and dihedral angles are shown in Fig. 1. Three methods of calculation were used to locate the TS of the reaction. There were no significant difference among the geometrical structures obtained by these calculation methods.

In the next stage, we tried to quantitatively analyze the endo-preference in the DA reactions. We first partitioned the activa-

Table 1. Experimental and Calculated Activation Energies in the Diels–Alder Reactions of 1,3-Cyclopentadiene (CP) with Maleic Anhydride (MA) (kcal/mol)

Cycloadduct endo or exo	Exp. data	Activation energy (ΔE_{act})/Calculation method[a)]						
		AM1	PM3	PM5	RHF//PM5[b)]	RHF//opt[c)]	B3LYP//PM5[b)]	B3LYP//opt[c)]
3endo	12.3[d)]	25.48	30.67	13.71	36.65	31.81	17.67	13.69[e)]
3exo	13.7[d)]	24.43	30.69	15.99	37.15	34.09	17.76	15.09
$\Delta\Delta E_{endo-exo}$	−1.4	1.05	−0.02	−2.28	−0.50	−2.28	−0.09	−1.40

a) The basis set of RHF and B3LYP methods is 6-31+G(d). b) RHF//PM5 and B3LYP//PM5 stand for the single-point calculation for the PM5 geometry. c) RHF//opt and B3LYP//opt stand for the reoptimization for the PM5 geometry. d) The data are from endo/exo = 91:9 at 298 K in Ref. 3. e) $E_{TS} - (E_{CP} + E_{MA})$. For example, $E_{TS(CP+MA)} - (E_{CP} + E_{MA}) = -573.394817 - ((-194.110328) + (-379.306312)) = 0.021823$ (au) = 13.69 (kcal/mol).

tion energies (ΔE_{act}) into diene deformation energy ($\Delta E_{df\text{-}dien}$), dienophile deformation energy ($\Delta E_{df\text{-}dphil}$) and diene–dienophile interaction energy (E_{int}) by PM5 and B3LYP methods, in which E_{int} is given by the following equation: $E_{int} = \Delta E_{act} - (\Delta E_{df\text{-}dien} + \Delta E_{df\text{-}dphil})$. Table 2 shows the deformation energies for dienophile, as well as the interaction energy for both exo and endo reactions. The values of $E_{df\text{-}dphil}$ for the exo reaction are 0.64, 0.7 kcal/mol higher than that for the endo by both PM5 and B3LYP respectively, which means that former reaction is more stressed or more strained than the endo reaction. This is clearly reflected in the interaction energy of reactions, where the endo E_{int} was 0.84 kcal/mol larger than the exo E_{int} in both methods of calculations. The analyses on the transition state points performed by PM5 and B3LYP methods reveal that the main factor controlling the endo-preference may be E_{int}, along with the deformation energy of the dienophile. The PM5 method was improved by introduction of effective core–core repulsion and van der Waals parameters.[18] This brings about the successive interpretation for reaction processes.

In an effort to understand clearly the role of the interaction energy, and its contribution in controlling the endo/exo selectivity, we partitioned the entire energy (ΔE_{irc}) along the intrinsic reaction coordinate (IRC) curve into $\Delta E_{df\text{-}dien}$, $\Delta E_{df\text{-}dphil}$, and E_{int}, on each IRC points as shown in Fig. 2. The clear ΔE_{irc}, $\Delta E_{df\text{-}dien}$, $\Delta E_{df\text{-}dphil}$, and E_{int} curves for endo/exo selectivity analysis are shown in Figs. 3–6. The endo-preference of ΔE_{irc} up to the transition state (ΔE_{act}) can be recognized to be supported by the endo-preferences of $E_{df\text{-}dien}$, $E_{df\text{-}dphil}$, and E_{int}, which are caused by the second orbital interaction (SOI). The exo-product preference after TS point is inferred to be caused

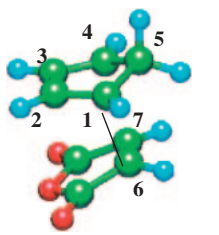

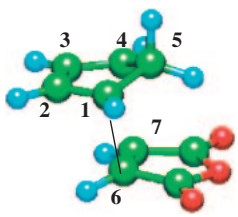

	endo		exo	
	1-6(Å)	2-1-4-5(degree)	1-6(Å)	2-1-4-5(degree)
PM5	2.157	154.2	2.173	152.9
B3LYP	2.217	151.6	2.238	151.8
RHF	2.186	150.1	2.210	150.7

Fig. 1. Optimized geometry distances and dihedral angles (2–1–4–5) at the transition states of the Diels–Alder reactions calculated by PM5, B3LYP//opt, and RHF//opt methods.

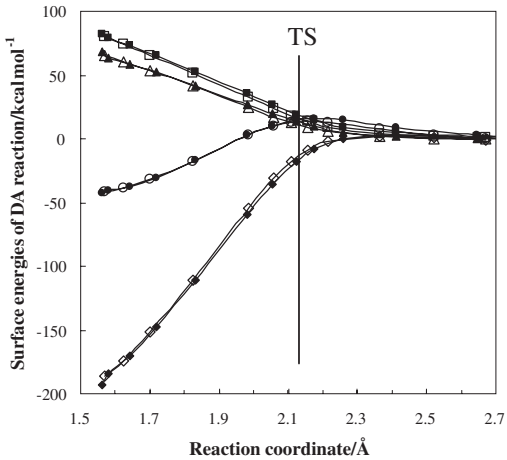

Fig. 2. Deformation energy analysis of the intrinsic reaction coordinate surface energy (ΔE_{irc}) in the DA reactions of CP with MA. $\Delta E_{irc(endo\ or\ exo)} = \Delta E_{df\text{-}dien} + \Delta E_{df\text{-}dphil} + E_{int}$. $\Delta E_{act} = E_{irc}$ at the transition state. ○: $\Delta E_{irc(endo)}$, ●: $\Delta E_{irc(exo)}$, □: $\Delta E_{df\text{-}dien(endo)}$, ■: $\Delta E_{df\text{-}dien(exo)}$, △: $\Delta E_{df\text{-}dphil(endo)}$, ▲: $\Delta E_{df\text{-}dphil(exo)}$, ◇: $E_{int(endo)}$, ◆: $E_{int(exo)}$.

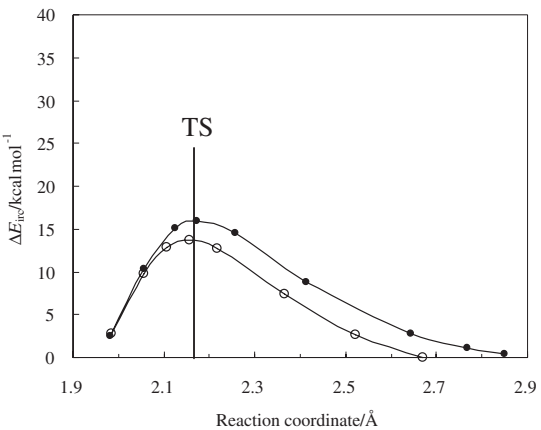

Fig. 3. Comparison between $\Delta E_{irc(endo)}$ and $\Delta E_{irc(exo)}$ in the DA reactions of CP with MA. ○: $\Delta E_{irc(endo)}$, ●: $\Delta E_{irc(exo)}$.

Table 2. Partitioning the Activation Energy (ΔE_{act}) into the Diene and Dienophile Deformation Energies ($\Delta E_{df\text{-}dien}$, $\Delta E_{df\text{-}dphil}$) and the Interaction Energy (E_{int}) in the Diels–Alder Reactions of CP with MA by PM5 and (B3LYP/6-31+G(d)) Methods

Product selectivity	ΔE_{act}	DA deformation energies/kcal mol^{-1}		
		$\Delta E_{df\text{-}dien}$	$\Delta E_{df\text{-}dphil}$	E_{int}
3endo	13.71	13.60	8.95	−8.84
	(13.69)	(16.81)[a)]	(10.31)	(−13.42)
3exo	15.99	14.40	9.59	−8.00
	(15.09)	(16.66)	(11.01)	(−12.58)
$\Delta\Delta E_{endo-exo}$	−2.28	−0.80	−0.64	−0.84
	(−1.40)	(0.15)	(−0.70)	(−0.84)

a) By B3LYP/6-31+G(d) level data. $\Delta E_{df\text{-}dien} = E_{TS\text{-}dien} - E_{dien} = -194.083543 - (-194.110328) = 0.026785$ au $= 16.81$ kcal/mol.

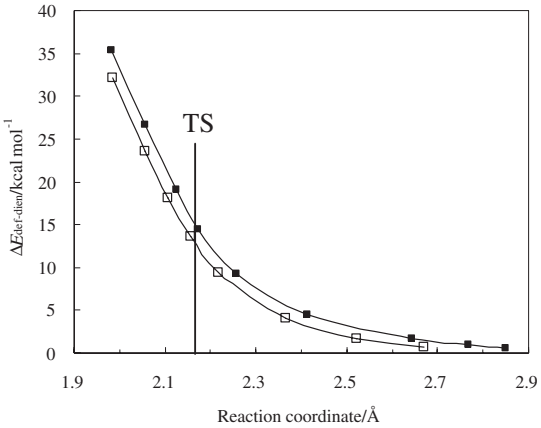

Fig. 4. Comparison between $\Delta E_{df\text{-}dien(endo)}$ and $\Delta E_{df\text{-}dien(exo)}$ in the DA reactions of CP with MA. □: $\Delta E_{df\text{-}dien(endo)}$, ■: $\Delta E_{df\text{-}dien(exo)}$.

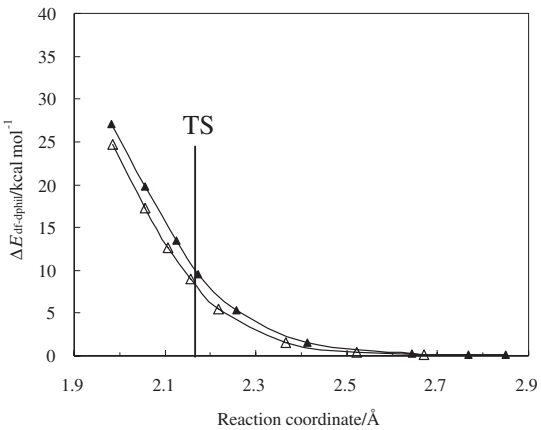

Fig. 5. Comparison between $\Delta E_{df\text{-}dphil(endo)}$ and $\Delta E_{df\text{-}dphil(exo)}$ in the DA reactions of CP with MA. △: $\Delta E_{df\text{-}dphil(endo)}$, ▲: $\Delta E_{df\text{-}dphil(exo)}$.

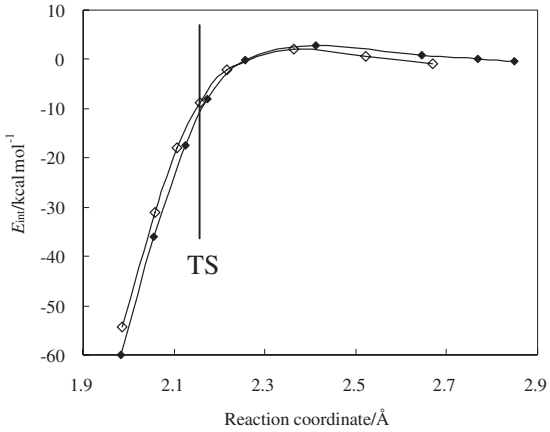

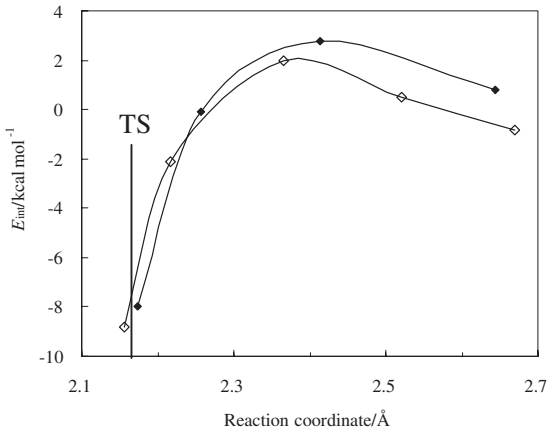

Fig. 6. Comparison between $\Delta E_{int(endo)}$ and $\Delta E_{int(exo)}$ in the DA reactions of CP with MA. ◇: $E_{int(endo)}$, ◆: $E_{int(exo)}$.

Table 3. Experimental and Calculated Activation Energies in the Diels–Alder Reactions of 5-Substituted 1,3-Cyclopentadienes with Acrylonitrile (kcal/mol)

Substituent	Cycloadduct	Exp. data	Activation Energy (ΔE_{act}) [kcal mol^{-1}]/Calculation method				
			PM3	PM5	RHF[a)]	B3LYP[a)]	B3LYP[b)]
H	**6** endo	15.2[c)]	32.95	22.52	37.50	18.31	20.49
	6 exo		32.71	22.51	37.55	18.07	20.03
F	**7a** syn	syn selective[d)]	31.14	20.01	32.93	13.47	15.24
	8a anti		33.63	23.46	39.46	18.51	20.37
Me	**7b** syn		34.31	24.56	39.98	20.00	20.66
	8b anti	anti selective[d)]	33.48	22.84	39.26	19.34	21.54

a) The basis set is 6-31+G(d) and the calculation was reoptimized by the method. b) The single-point calculation is performed B3LYP/6-31+G(d) for the PM5 geometry. c) The experimental data are shown in Refs. 8 and 21. d) The experimental data are shown in Ref. 22.

by the exo-preference of ΔE_{irc} and E_{int}, which may be connected with larger repulsions for the endo-pathway. In the final stage of the reaction (adduct formation), the exo product was 1.26 kcal/mol lower than the endo product at the B3LYP level of calculation. This energy difference is reasonable, since the endo structure is more strained than the exo structure.

DA Reactions of 5-Substituted CP with Acrylonitrile (AN). We next studied the syn/anti facial selectivity of the DA reactions between 5-substituted 1,3-cyclopentadienes (**4a**; X = F, **4b**; X = Me) and AN (**5**). As shown in Scheme 2, the main product of the reaction between **4a** and **5** is a syn-endo adduct (**7a**), while the main product is an anti-endo adduct (**8b**)

for the reaction between **4b** and **5**.[21] Table 3 shows the activation energies calculated using various methods for possible stereoisomeric additions of **1** + **5**, **4a** + **5**, and **4b** + **5** reactions, respectively. The syn-selectivity of the 5-F-CP reaction and the anti-selectivity of the 5-Me-CP reaction were explained by four methods of calculations. Activation energy barriers of the main selective products are inferred to be smaller than the E_{act} for the adjacent isomers. PM5 and B3LYP activation energy values are in better agreement with the experimental results than the values from PM3 and RHF calculations. We thus intend to reveal the origin of the facial selectivity using the B3LYP and the economical PM5 methods. It is worth mentioning that the PM5 method afforded relatively good ΔE_{act} results concerning the symmetrical diene reaction. The PM5 and B3LYP methods

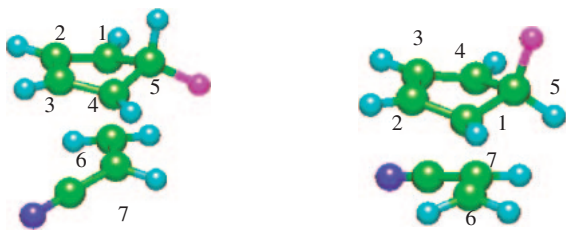

7a 8a

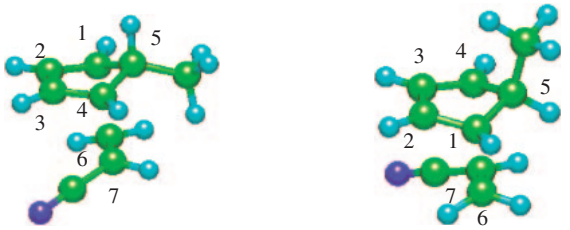

7b 8b

		1-6(Å)	4-7(Å)	2-1-4-5
7a	syn	2.03	2.24	-148.9
		(2.12)	(2.48)	(-149.9)
8a	anti	2.02	2.26	152.5
		(2.10)	(2.53)	(154.8)
7b	syn	2.02	2.28	-149.4
		(2.08)	(2.51)	(-151.1)
8b	anti	2.01	2.27	151.9
		(2.08)	(2.23)	(150.8)

Fig. 7. Optimized geometry structures at the DA transition states calculated by PM5 and (B3LYP/6-31+G(d)) methods.

were used to locate the transition state structures corresponding to the four possible cycloadditions between 5-F-CP or 5-Me-CP and acrylonitrile, as shown in Fig. 7. The reactions of unsymmetrical dienes with dienophiles necessarily involve unsymmetrical transition states. The two forming bonds of C1–C6 and C4–C7 do not have the same length at TS. Therefore, we predict an asynchronous concerted transition state for these reactions. This can be recognized graphically by the PM5 method.

We tried to probe more clearly the role of deformation energies in controlling the selectivity preference. The activation energies (ΔE_{act}) were partitioned into the diene ($\Delta E_{df\text{-}dien}$) and dienophile ($\Delta E_{df\text{-}dphil}$) deformation energies and the diene–dienophile interaction energies (E_{int}). The equation can be described as follows: $\Delta E_{act} = \Delta E_{df\text{-}dien} + \Delta E_{df\text{-}dphil} + E_{int}$. According to the 5-F-CP reaction, the dien-deformation has shown a vital role in the reaction selectivity. The resulted calculations are shown in Table 4. We inferred that the syn-selectivity is preferred over the anti-selectivity for this reaction due to the lower energy (14.68 kcal/mol for 18.23 kcal/mol) required to deform the dien into its TS structure by the 5-syn-F group; this in turn may cause lesser repulsion E_{int} between the reacted species. Another conclusion can be applied to the reaction of 5-Me-CP. In this case, the anti-selectivity is inferred to be caused by intra- and intermolecular repulsions by the 5-syn-Me group of the syn-isomer. The reactions of the substituted CP can be compared with those of the symmetrical CP more clearly since all the reactions afforded endo-selectivity.

For further analysis of the substituted CP reactions, we partitioned the entire energy (ΔE_{irc}) along the intrinsic reaction coordinate (IRC) curve into $\Delta E_{df\text{-}dien}$, $\Delta E_{df\text{-}dphil}$, and E_{int} (Figs. 8 and 9). Figure 8 clearly shows that the syn-selectivity in the case of 5-F-CP comes from the smaller $\Delta E_{df\text{-}dien}$ and better E_{int} between the reactants. In the same way, the anti-selectivity of 5-Me-CP was explained, since the $E_{df\text{-}dien}$ for the syn-selectivity was less in Fig. 9. We believe that this trend of the larger syn-selectivity comes from the intramolecular π_{homo}–n_F orbital mixing of 5-F-CP[5] and from the intermolecular interactions of the induced larger diene-π orbital with acrylonitrile.

Conclusion

The origin of typical stereoselective DA reactions of 5-substituted CP with two kinds of dienophiles, MA and AN, was analysed by calculation of the activation energies (ΔE_{act}), and the partition to the deformation energies ($\Delta E_{df\text{-}dien}$, $\Delta E_{df\text{-}dphil}$) and interaction energy (E_{int}) using improved PM5 and B3LYP/6-

Table 4. Partitioning of the Activation Energy into Diene and Dienophile Deformation Energies and the Interaction Energy for Diels–Alder Reactions of 5-Substituted 1,3-Cyclopentadiene (CP) with Acrylonitlile by PM5 Method

Substituent	Product selectivity	ΔE_{act}	Deformation energy/kcal mol^{-1}		
			$\Delta E_{df\text{-}dien}$	$\Delta E_{df\text{-}dphil}$	E_{int}
H	**6** endo	22.52	15.48	10.00	−2.96
F	**7a** syn[a)]	20.01	14.68	9.37	−4.04
	8a anti	23.46	18.23	9.59	−4.36
Me	**7b** syn	24.57	17.44	9.42	−2.29
	8b anti[a)]	22.86	15.87	9.81	−2.82

a) The main adduct.

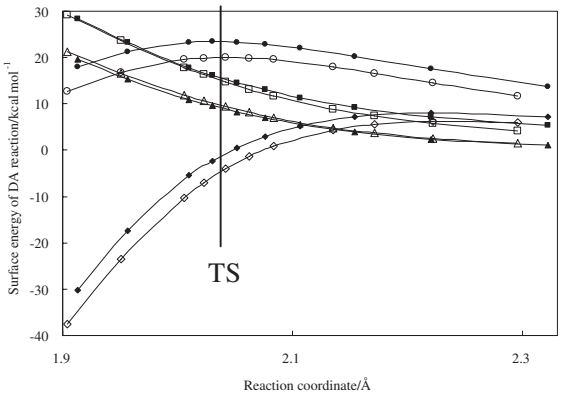

Fig. 8. Deformation energy analysis of the intrinsic reaction coordinate surface energy (E_{irc}) into the three components ($\Delta E_{df\text{-}dien}$, $\Delta E_{df\text{-}dphil}$, E_{int}) in the two DA reactions between 5-F-CP and AN. $\Delta E_{irc(syn\ or\ anti)} = \Delta E_{df\text{-}dien} + \Delta E_{df\text{-}dphil} + E_{int}$. $\Delta E_{act} = E_{irc}$ at the transition state. ○: $\Delta E_{irc(syn)}$, ●: $\Delta E_{irc(anti)}$, □: $\Delta E_{df\text{-}dien(syn)}$, ■: $\Delta E_{df\text{-}dien(anti)}$, △: $\Delta E_{df\text{-}dphil(syn)}$, ▲: $\Delta E_{df\text{-}dphil(anti)}$, ◇: $E_{int(syn)}$, ◆: $E_{int(anti)}$.

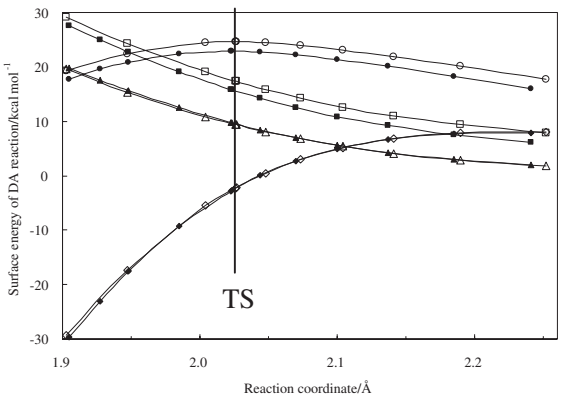

Fig. 9. Deformation energy analysis of the intrinsic reaction coordinate surface energy (E_{irc}) into the three components ($\Delta E_{df\text{-}dien}$, $\Delta E_{df\text{-}dphil}$, E_{int}) in the two DA reactions between 5-Me-CP and AN. $\Delta E_{irc(syn\ or\ anti)} = \Delta E_{df\text{-}dien} + \Delta E_{df\text{-}dphil} + E_{int}$. $\Delta E_{act} = E_{irc}$ at the transition state. ○: $\Delta E_{irc(syn)}$, ●: $\Delta E_{irc(anti)}$, □: $\Delta E_{df\text{-}dien(syn)}$, ■: $\Delta E_{df\text{-}dien(anti)}$, △: $\Delta E_{df\text{-}dphil(syn)}$, ▲: $\Delta E_{df\text{-}dphil(anti)}$, ◇: $E_{int(syn)}$, ◆: $E_{int(anti)}$.

31+G(d) methods. We also newly partitioned each point on the intrinsic reaction coordinate (IRC) surface energy (ΔE_{irc}) to two reactant deformation energies and the interaction energy for more clear analysis. The syn-selectivity of the 5-F-CP comes from the lower ΔE_{act} (2–3 kcal/mol) caused by relatively smaller $E_{df\text{-}dien}$ and smaller E_{int}, which leads to smaller repulsion. These low energies are inferred to be caused by larger intramolecular n–π orbital interactions between the diene π and F-n orbital moieties, and by the larger intermolecular π–π orbital interactions between the larger diene-π orbital and dienenophile-π orbital moieties. The anti-selectivity of the 5-Me-CP comes mainly from larger $E_{df\text{-}dien}$ values at the syn-isomer. The new, effective and economical method of the IRC energy partitioning to the reactants, TS intermediates and products, may be also introduced to verify the energy balance of other calculation methods and other reactions. The method may also provide much valuable information to help to analyze the reaction mechanism.

We thank Dr. K. Sameshima at software of Fujitsu com. for the excellent support.

References

1 a) R. B. Woodward and R. Hoffman, *Angew. Chem., Int. Ed. Engl.*, **8**, 781 (1969). b) W. Carruthers, "Cycloaddition Reactions in Organic Synthesis," Pergamon Press, Oxford, Great Britain (1990).

2 F. Fringuelli and A. Taticchi, "Dienes in the Diels–Alder Reactions," John Wiley & Sons, New York (1990).

3 A. Arrieta and F. P. Cossio, *J. Org. Chem.*, **66**, 6178 (2001).

4 M. Ishida, M. Sakamoto, H. Hattori, M. Shimizu, and S. Inagaki, *Tetrahedron Lett.*, **42**, 3471 (2001).

5 M. Ishida, S. Hirasawa, and S. Inagaki, *Tetrahedron Lett.*, **44**, 2187 (2003).

6 J. D. Xidos, R. A. Poirier, C. C. Pye, and D. J. Burnell, *J. Org. Chem.*, **63**, 105 (1998).

7 a) E. Goldstein, B. Beno, and K. N. Houk, *J. Am. Chem. Soc.*, **118**, 6036 (1996). b) S. Yamabe, "Frontier Orbital Theory and Its Application (Kagaku Sousetu No. 46)," ed by S. Tokita, Nippon Kagaku Kai, Tokyo (2000), pp. 31–40. c) S. Sakaki, "Reasonable Design of Chemical Reactions Based on Theoretical Calculation (Kagaku Sousetsu No. 47)," ed by S. Murai, Nippon Kagaku Kai, Tokyo (2000), pp. 179–193.

8 L. R. Domingo, M. J. Aurell, P. Pere, and R. Contreras, *J. Org. Chem.*, **68**, 3884 (2003).

9 R. A. King, T. D. Crawford, J. F. Stanton, and H. F. Schaefer, III, *J. Am. Chem. Soc.*, **121**, 10788 (1999).

10 S. C. Pellegrinet, M. T. Baumgartner, R. A. Spanevello, and A. B. Pierini, *Tetrahedron*, **56**, 5311 (2000).

11 L. R. Domingo, M. Oliva, and J. Andres, *J. Org. Chem.*, **66**, 6151 (2001).

12 K. Afarinkia, M. J. Bearpark, and A. Ndibwami, *J. Org. Chem.*, **68**, 7158 (2003).

13 a) T. Suishu, T. Obata, T. Shimo, and K. Somekawa, *Nippon Kagaku Kaishi*, **2000**, 167. b) T. Shimo and K. Somekawa, "CRC Handbook of Organic Photochemistry and Photobiology," ed by W. Horspool and F. Lenci, CRC Press, London (2003), pp. 82-1–82-19.

14 T. Shimo, T. Uezono, T. Obata, M. Yasutake, T. Shinmyouzu, and K. Somekawa, *Tetrahedron*, **58**, 6111 (2002).

15 H. I. Omar, Y. Odo, Y. Shigemitsu, T. Shimo, and K. Somekawa, *Tetrahedron*, **59**, 8099 (2003).

16 J. M. Coxon, S. T. Grice, R. G. A. R. Maclagan, and D. Q. McDonald, *J. Org. Chem.*, **55**, 3804 (1990).

17 J. J. P. Stewart, *Int. J. Quantum. Chem.*, **58**, 133 (1996).

18 J. J. P. Stewart, "WinMOPAC V3.5," Fujitsu Ltd., Tokyo, Japan (2001).

19 A. Frisch and M. J. Frsch, "Gaussian 98," Gaussian Inc., Pittsburgh (1998).

20 a) A. D. Becke, *J. Chem. Phys.*, **98**, 5648 (1993). b) C. Lee, W. Yang, and R. C. Parr, *Phys. Rev. B*, **37**, 785 (1998).

21 J. Sauer, H. Wiest, and A. Mielert, *Chem. Ber.*, **97**, 3183 (1964).

22 a) S. D. Kahn and W. J. Hehre, *J. Am. Chem. Soc.*, **109**, 663 (1987). b) W. J. Hehre, L. D. Burke, A. J. Shusterman, and W. J. Pietro, "Experiments in Computational Organic Chemistry," Wavefunction Inc., California (1993), Chap. 5.